

# High-resolution resonant photoemission study of the 4f states in a typical Kondo system: CePd<sub>3</sub>

M. Zacchigna<sup>1</sup>, J. Almeida<sup>1</sup>, I. Vobornik<sup>1</sup>, G. Margaritondo<sup>1</sup>, D. Malterre<sup>2</sup>, B. Malaman<sup>2</sup>, and M. Grioni<sup>1,a</sup>

<sup>1</sup> Institut de Physique Appliquée, École Polytechnique Fédérale, 1015 Lausanne, Switzerland

<sup>2</sup> Université H. Poincaré, 54506 Vandœuvre, France

Received: 13 October 1997 / Accepted: 21 January 1998

**Abstract.** We exploited resonant photoemission at the Ce 4d → 4f absorption edge to investigate the Ce 4f states in CePd<sub>3</sub>. High resolution spectra reveal, near the Fermi level, the characteristic fine structure of intermediate valence Ce compounds. The spectral lineshape is consistent with the typical “Kondo” character of CePd, but the prominent (f<sup>0</sup>) ionization peak is found at the unusually low binding energy of 1 eV. We briefly discuss the implications of these observations.

**PACS.** 71.28.+d Narrow-band systems; intermediate-valence solids – 78.90.+t Other topics in optical properties, condensed matter spectroscopy and other interactions of particles and radiation with condensed matter – 79.60.-i Photoemission and photoelectron spectra

## 1 Introduction

Intermediate valence cerium compounds have been much studied as model systems where electronic correlations induce a variety of unusual physical properties [1]. Their “Kondo behavior” is the result of a delicate balance between two competing factors. On one hand, the strong on-site Coulomb repulsion favors localization of one 4f electron per Ce site. On the other end, the 4f electrons tend to delocalize by hybridizing with the itinerant conduction electrons. Conventional band theory is inadequate to describe this complex dynamical problem, and simplified models provide a better physical insight. The celebrated Anderson Impurity Model (AIM) captures an essential aspect of the physics of these materials, namely the crossover from local moments, to a low-temperature Fermi liquid regime, where the moments are quenched. Despite its limitations, the AIM remains an inescapable reference, because the extension to a lattice model has proven a formidable task.

Electron spectroscopies, especially photoemission (PES) and Inverse Photoemission (IPES), have given precious clues to the Kondo problem. The impurity model provides a framework to interpret the clear fingerprints of electronic correlations observed in the valence band and core level spectra. According to approximate solution of the AIM, the characteristic low energy features in the Ce 4f spectrum reflect the emerging small energy scale  $\delta = k_B T_K$  (where  $T_K$  is Kondo temperature) of the impurity problem. Satellites in the core level spectra reveal the large energy scales (Coulomb repulsion, hybridization),

and the configuration mixing [2,3]. Spectroscopic data can therefore be used to test the consistency of the model, and to estimate its parameters. Several experiments have revealed a good qualitative agreement with the AIM predictions [4], but differences have been found at a quantitative level. The possibility that these discrepancies may indicate some different and new physics, *e.g.* coherence effects, is a matter of current debate [5–7].

The experimental spectra of Ce based materials contain overlapping contributions from the various elements and orbital symmetries. It is often difficult to accurately determine the 4f signal especially for compounds with the transition metals (TM), where the TM d band dominates the emission from the single Ce 4f electron. Resonances of the 4f cross section at the Ce 4d – 4f or 3d – 4f absorption edges, can be exploited to enhance the 4f signal. The use of resonant PES (RESPES) in the Ce problem has been reviewed in reference [8]. The complementary resonant IPES (RIPES) has also been demonstrated [9,10]. With recent advances in synchrotron radiation instrumentation, high energy resolution experiments are finally possible, and the potential of RESPES can be fully exploited [11,12].

CePd<sub>3</sub> is a typical Kondo system. Transport [13] and magnetic [14] measurements suggest a moderately strong 4f-band hybridization, with  $T_K \sim 350$  K, which puts CePd<sub>3</sub> in the so-called “Kondo regime” of the AIM. Inelastic neutron scattering data [15] reveal a very good agreement with an impurity spectral function, with  $T_K \sim 600$  K. A more “exotic” behavior is suggested by recent optical measurements by Bucher *et al.* [16]. They observe an anomalous temperature-dependent spectral weight transfer from low to high ( $\sim 1$  eV) energies, which

<sup>a</sup> e-mail: grioni@dpmail.epfl.ch

they interpret as the opening of a deep pseudogap around  $E_F$ , and suggest that  $\text{CePd}_3$  should be viewed as a lightly doped Kondo insulator. Core level spectra confirm the moderately hybridized character of the 4f states [17]. Conventional valence band spectra of this material are characteristically insensitive to the 4f electrons. Early RESPES data [18–20] have identified a 4f emission up to the Fermi level but, due to the limited energy resolution, could not reveal any fine structure.

In this paper we present new high resolution RESPES measurements which, combined with recent RIPES results, yield a clear picture of the 4f states in  $\text{CePd}_3$ . We show that the observed spectral signatures, namely the characteristic fine structure near the Fermi level, are consistent with the physical properties of  $\text{CePd}_3$ . We also show that the bare 4f energy is unusually small in this material. Since alternative descriptions [21,22] of Ce intermediate-valence materials have not been worked out in sufficient detail for a comparison with experiment, we will base the discussion of the experimental data on the AIM approach.

## 2 Experimental

Polycrystalline samples of  $\text{CePd}_3$  were prepared by melting stoichiometric amounts of the components in an induction furnace. Powder X-ray diffraction indicated that any spurious phases, if present, represented less than 1% of the total volume. We measured the Ce 4d–4f RESPES spectra at the VUV undulator beamline of the ELETTRA storage ring. The samples were mounted on a closed-cycle refrigerator, and held at a temperature of 40 K, and fresh surfaces were prepared by scraping with a diamond file at a base pressure of  $1 \times 10^{-10}$  torr. Valence band spectra were collected by a 150 mm mean-radius hemispherical analyzer. The total energy broadening (electrons + photons) was 40 meV in the 110–120 eV photon energy range. It was determined from the width of the metallic Fermi edge of the off-resonance spectra, where the 4f contribution is negligible. We also measured valence band and Ce 3d core level spectra with a monochromatized Al  $K_\alpha$  ( $h\nu = 1486$  eV) rotating anode source and a Scienta ESCA-300 analyzer, in Lausanne. The total energy resolution for these measurements was 300 meV.

## 3 Results and discussion

Figure 1 shows valence band PES spectra of  $\text{CePd}_3$  at various photon energies, from  $h\nu = 40.8$  eV (He II) to 1486 eV (Al  $K_\alpha$ ). The HeII and Al  $K_\alpha$  spectra are quite similar, apart from a larger instrumental broadening in the latter. They are dominated by emission from the Pd d band at  $-2.5$  eV and  $-4$  eV [23], as expected from the atomic cross sections for the Pd 5d and Ce 4f states [24]. The d band also dominates the first spectrum in the resonance region ( $h\nu = 112$  eV). The larger intensity of the  $-4$  eV peak at 112 eV may reflect the energy dependence of the cross

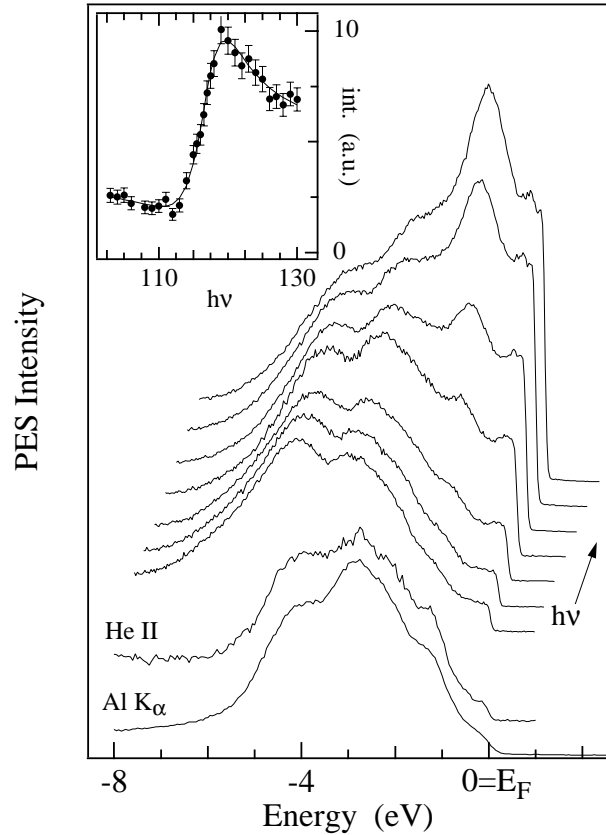


**Fig. 1.** Valence band PES spectra of  $\text{CePd}_3$  at selected energies (first: 112 eV, last 120 eV) across the 4d – 4f giant resonance. The spectra have been arbitrarily normalized at  $-8$  eV, and offset for clarity. Also shown are HeII (40.8 eV) and Al  $K_\alpha$  (1486 eV) spectra. Inset: Photon energy dependence of the PES intensity at  $-1$  eV. The line is a fit with a Fano lineshape.

sections, although a small residual surface contamination, at sub-monolayer level, could contribute to the intensity at this energy. The emission at  $E_F$  is small but finite, in agreement with the metallic character of  $\text{CePd}_3$ , and with indication of a pseudogap from optics [16]. These spectra do not show any clear 4f features. An unambiguous determination of the 4f signal is only possible by following the evolution across the 4d – 4f resonance.

With increasing photon energy a prominent peak develops at  $-1$  eV, and additional emission appears within 0.5 eV of  $E_F$ . The photon energy dependence of the total PES intensity at  $-1$  eV, in the inset of Figure 1, exhibits a clear resonance, and it is possible to fit a Fano lineshape to these data points. This energy dependence identifies the 1 eV peak as a Ce 4f feature. Within the AIM this peak is the “ionization” peak of mainly “f $^0$ ” character. Its energy, apart from small hybridization shifts, is equal to the “bare” 4f energy  $\varepsilon_f$ . The observed value is smaller than previous determinations [18–20]. It is also considerably smaller than in other typical Kondo systems, where  $|\varepsilon_f| = 1.5 - 2$  eV. Similar values have been found in mixed-valence materials like  $\text{CePd}_7$  [25], where a strong 4f-band hybridization yields Kondo temperatures

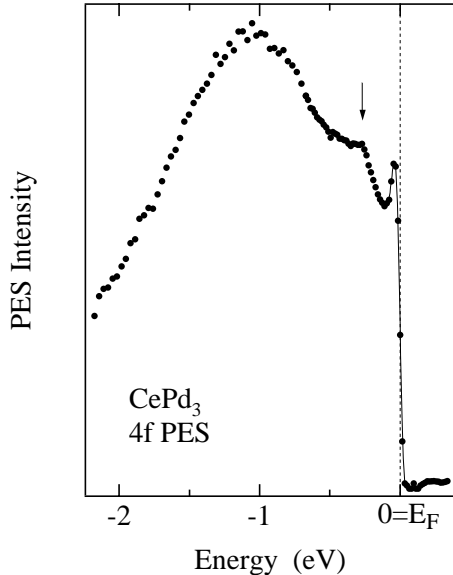


**Fig. 2.** Experimental Ce 4f PES spectral function, obtained by subtracting high resolution on- and off-resonance spectra. The broad feature at  $-1$  eV is the (“ $f^0$ ”) ionization peak. The resolution-limited feature at  $E_F$  is the tail of the Kondo resonance. The arrow indicates the spin-orbit satellite.

in excess of 1000 K, and 4f occupation numbers  $n_f < 0.8$ . The present result is therefore rather surprising.

The Kondo scenario for Ce compounds predicts that, besides the atomic-like  $f^0$  peak, new 4f structures should appear near  $E_F$ . These features are a consequence of hybridization, and have intrinsically a many-body character. We can identify both large- and small-energy-scale 4f features in the difference spectrum of Figure 2, obtained by subtracting high resolution on- and off-resonance spectra. This spectrum, which essentially represents the 4f states, is dominated by the  $f^0$  peak at  $-1$  eV. It also exhibits a sharp peak near the Fermi level, and a satellite at  $-0.3$  eV. The position and width of the leading peak are resolution limited, and consistent with the presence of a sharp feature just above  $E_F$ , cut by the Fermi-Dirac function. The AIM interprets this peak as the tail of the mostly unoccupied Kondo resonance, at  $k_B T_K$  above  $E_F$ , and the  $-0.3$  eV feature as a spin-orbit satellite. The relative intensities of the “Kondo” and ionization peak, and of the “Kondo” and spin-orbit satellite, in the spectrum of Figure 2, are typical of a moderately hybridized Ce compound [26].

Combined PES/IPES data yield a complete picture of the electronic structure of CePd<sub>3</sub>. The PES and IPES spectra of Figure 3 have been drawn, as usual, on opposite sides of the common Fermi level. The PES spectra are the on- and off-resonance spectra of Figure 1. The IPES spectra have been measured at excitation energies close to the 3d – 4f resonance [10]. At variance with conventional IPES spectra ( $h\nu = 1486$  eV), where the d and 4f features have comparable intensities [4], the sensitivity of the RIPES spectra to the unoccupied 4f states can be greatly changed by an appropriate choice of the excitation energy. The shaded spectrum corresponds to the minimum

**Table 1.** Parameter values used in the modified AIM calculation of the IPES and Ce 3d spectra.  $\varepsilon_f$  is the bare 4f energy;  $U_{ff}$  is the on-site 4f Coulomb repulsion;  $V_1$  is the hybridization associated with the  $4f^1$  configuration;  $U_{fc}$  is the core hole-4f Coulomb attraction;  $R = V_n/V_{n+1}$ , where  $n$  and  $n+1$  are the occupation numbers of the relevant configurations.

	$\varepsilon_f$ (eV)	$U_{ff}$ (eV)	$V_1$ (eV)	$U_{fc}$ (eV)	$R$
Ground State and IPES	$-1.0$	$5.3$	$0.3$	$-$	$0.65$
Ce 3d XPS	$-1.0$	$7.4$	$0.24$	$11.0$	$0.65$

of the 4f IPES cross section, and only shows the unoccupied d band. The second IPES spectrum, collected near resonance, essentially reflects 4f states [27]. Within the AIM the broad peak just above  $E_F$  reflects the unoccupied part of the Kondo resonance, and an unresolved spin-orbit satellite. The second peak at higher energy is the affinity ( $f^2$ ) peak. We conclude that the non-f (shaded) part of the spectral function of CePd<sub>3</sub> exhibits a broad ( $\sim 3$  eV) and deep pseudogap around  $E_F$ . The  $f^0$  and “Kondo” part of the 4f spectrum develop in this pseudogap.

We have already mentioned that the  $\varepsilon_f$  value obtained from the resonance data of Figures 1 and 2 is unusually small for a typical Kondo system like CePd<sub>3</sub>. We have performed calculations of the IPES, and of the Ce 3d spectral functions to investigate whether this value is compatible with an AIM description of the spectral properties. The calculations are based on an extension of the Gunnarsson-Schönhammer (GS) variational approach to the AIM [2]. Unlike the original GS model, our computer code allows for the possibility of using different hybridization parameters for the different relevant 4f configurations. This configuration-dependent-hybridization approach is based on calculations by Gunnarsson and Jepsen [28] and, as discussed in reference [29], it is necessary for a quantitative description of the spectroscopic measurement. The different hybridization parameters result from changes in the spatial extension of the 4f wavefunction due to changes in the 4f occupation number, and/or to the presence of a core hole in the final state.

The lineshape, and relative intensity of the 4f structures in the IPES spectrum strongly depends on the excitation energy near resonance [27]. Therefore we have only performed calculations for conventional (non-resonant) IPES. The experimental and calculated IPES spectra are compared in Figure 4, and the parameters used in the calculation are shown in Table 1. As in reference [30], the inelastic background and the non-f signal have been modeled by the spectrum of YPd<sub>3</sub>, a material with a similar band structure but no 4f electrons. We have neglected the crystal field splitting of the  $J = 5/2$  manifold, since CEF effects are small in this system [31]. The calculation well reproduces the position and the relative intensity of the 4f features.

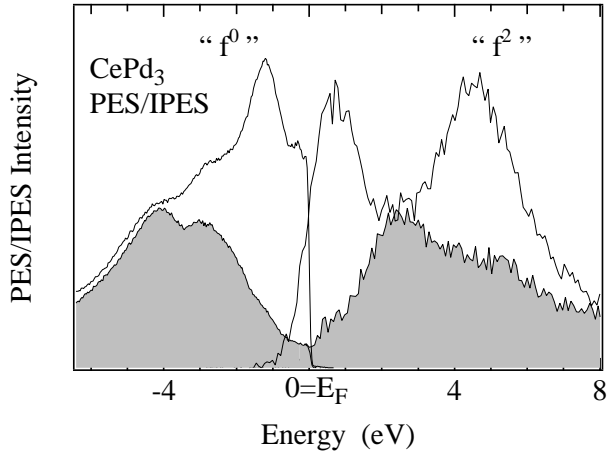


**Fig. 3.** Photoemission ( $E < 0$ ) and Inverse photoemission ( $E > 0$ ) spectra of  $\text{CePd}_3$ . The PES spectra are the off- and on-resonance spectra from Figure 1. The IPES spectra, from reference [10] have been measured near the 3d – 4f resonance. The off-resonance spectra (shaded curves) illustrate the non-4f density of states, which exhibits a deep pseudogap around  $E_F$ .

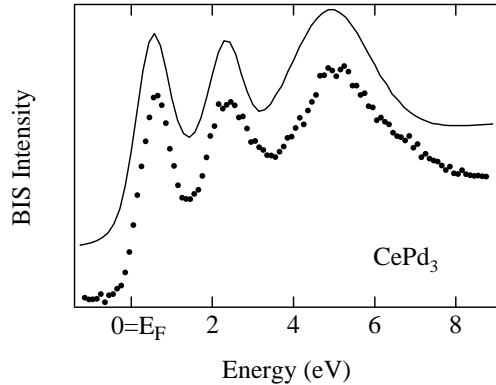


**Fig. 4.** Conventional IPES spectrum ( $h\nu = 1486$  eV) of  $\text{CePd}_3$  from reference [30], and the result of an AIM calculation. As in reference [30], an appropriate non-f and inelastic background has been added. The values of the parameters used in the calculation are shown in Table 1.

The Ce 3d core spectrum is shown in Figure 5. The lineshape is complex, with 6 partially overlapping features from 3 final state configurations ( $f^0$ ,  $f^1$  and  $f^2$ ), further split by the spin-orbit interaction. Again, all the experimental features are well reproduced by the calculation, including the intensity of the characteristic “ $f^0$ ” peak at 914 eV, a rather accurate indicator of hybridization in the ground state. The larger 4f Coulomb repulsion and smaller hybridization parameters in the final state, compared with the ground state values, are consistent with our previous experience [32].

In our calculations we have neglected the possibility of different surface and bulk contributions to the spectral

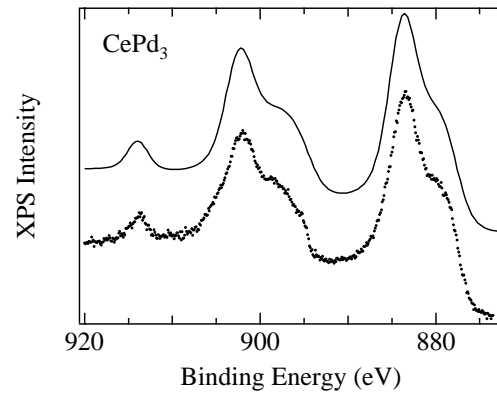


**Fig. 5.** Experimental Ce 3d XPS spectrum of  $\text{CePd}_3$ , compared with an AIM calculation. A Shirley background has been added to the calculated spectrum. The values of the parameters used in the calculation are shown in Table 1.

functions. The existence of a distinct surface signal, reflecting a different (smaller) hybridization from that characteristic of the bulk has been clearly demonstrated [33, 34], at least in strongly hybridized materials like  $\text{CeRh}_3$ . We have ignored these complexities, because we expect this effect to be less important in  $\text{CePd}_3$ . Also, we are mainly interested here in the consistency of an AIM description with the experimentally derived  $\varepsilon_f$  value. Even within these limits we can reach an interesting conclusion. We could obtain acceptable fits to the experimental Ce 3d and IPES (but not the PES) spectra with more standard values  $|\varepsilon_f| \sim 1.5 - 2$  eV [35]. However, this was only possible by increasing at the same time the hybridization value. The AIM result  $T_K \sim \exp(\pi\varepsilon_f/NV^2)$  shows that  $\varepsilon_f$  and the hybridization strength  $V$  have an opposite influence on  $T_K$ .  $V$  is essentially proportional to the density of conduction states (DOS) at the Fermi level. We therefore speculate that the typical Kondo behavior of  $\text{CePd}_3$ , is the result of an unusually small 4f bare energy, and a small DOS at  $E_F$ .

In summary, we have exploited resonant PES to identify the 4f states in  $\text{CePd}_3$ . In combination with RIPES data, these results provide a complete picture of the Ce 4f spectral function in this material. The observed lineshape is consistent with the typical Kondo character of  $\text{CePd}_3$ , and a simple impurity model description appears qualitatively adequate. Interestingly, this “typical” behavior results from two rather unusual circumstance: i) a “bare” 4f binding energy  $\varepsilon_f = -1$  eV considerably smaller than in materials similar physical properties, and more typical of strongly hybridized materials; ii) a density of states at the Fermi level smaller than in most Ce-TM intermetallics. Both these quantities enter, in opposite ways, in the expression for the Kondo temperature  $T_K$ , and apparently conjure to produce the observed moderate value of  $T_K$ . These experimental results should encourage a reevaluation of recent detailed calculations of the electronic structure of  $\text{CePd}_3$ , which assumed a more standard value  $\varepsilon_f = -2$  eV [31].

The spectroscopic results confirm the occurrence of a deep and broad pseudogap around the Fermi level, but do not reveal fine structures which could be associated with an underlying Kondo insulator character of CePd<sub>3</sub> [16]. We cannot of course exclude the existence of narrow gaps at particular locations of  $k$  space. A systematic high-energy resolution angle-resolved investigation of high-quality single crystal surfaces could clarify this important issue, and would represent a natural extension of the present work.

We gratefully acknowledge the competent assistance of the ELETTRA staff, and the collaboration of Dr. K. Prince. It is a pleasure to thank J. Sorel and F. Del Dongo for their critical remarks. This work has been supported by the Swiss National Science Foundation.

## References

1. A.C. Hewson, “*The Kondo problem to heavy fermions*” (Cambridge University Press, 1993) and references therein.
2. O. Gunnarsson, K. Schönhammer, Phys. Rev. B **28**, 4315 (1983).
3. N.E. Bickers, D.L. Cox, J.W. Wilkins, Phys. Rev. B **36**, 2036 (1987).
4. D. Malterre, M. Grioni, Y. Baer, Adv. Phys. **35**, 299 (1996).
5. J.J. Joyce *et al.*, Phys. Rev. Lett. **68**, 236 (1992).
6. A.J. Arko *et al.*, Physica B 230-232, **16** (1997).
7. M. Garnier *et al.*, Phys. Rev. Lett. **78**, 4127 (1997).
8. J.W. Allen *et al.*, Adv. Phys. **35**, 275 (1986).
9. P. Weibel *et al.*, Phys. Rev. Lett. **72**, 1252 (1994).
10. M. Grioni *et al.*, Phys. Rev. B **55**, 2056 (1997).
11. E. Weschke *et al.*, Phys. Rev. B **44**, 8304 (1991).
12. G. Chiaia *et al.*, Phys. Rev. B **55**, 9207 (1997).
13. E. Holland-Moritz, M. Loewenhaupt, W. Schmatz, D.K. Wohlleben, Phys. Rev. Lett. **17**, 983 (1977).
14. A. Qachaou *et al.*, J. Magn. Magn. Mat. **63-64**, 635 (1987).
15. A.P. Murani, R. Raphael, Z.A. Bowden, R.S. Eccleston, Phys. Rev. B **53**, 8188 (1996).
16. B. Bucher *et al.*, Phys. Rev. B **53**, R2948 (1996).
17. J.C. Fuggle *et al.*, Phys. Rev. B **27**, 7330 (1983).
18. J.W. Allen *et al.*, Phys. Rev. Lett. **46**, 1100 (1981).
19. R.D. Parks *et al.*, Phys. Rev. Lett. **52**, 2176 (1984).
20. F.U. Hillebrecht *et al.*, J. Magn. Magn. Mater. **47-48**, 221 (1985).
21. Q.G. Sheng, B.R. Cooper, Philos. Mag. Lett. **72**, 123 (1995).
22. A.N. Tahlvidar-Zadeh, M. Jarrel, J.K. Freericks, Phys. Rev. B **55**, 3332 (1997).
23. C. Koenig, M.A. Kahn, Phys. Rev. B **38**, 5887 (1988).
24. J.J. Yeh, I. Lindau, Atom. Data and Nucl. Data Tabl. **32**, 1 (1985).
25. Y. Iwamoto, M. Nakazawa, A. Kotani, J.C. Parlebas, J. Phys.: Condens. Matt. **7**, 1149 (1995).
26. F. Patthey *et al.*, Phys. Rev. B **42**, 8864 (1990).
27. A. Tanaka, T. Jo, J. Phys. Soc. Jpn. **65**, 615 (1996).
28. O. Gunnarsson, O. Jepsen, Phys. Rev. B **38**, 3568 (1988).
29. N. Witkowski, F. Bertran, D. Malterre, Phys. Rev. B **56**, 15040 (1997).
30. D. Malterre, M. Grioni, P. Weibel, B. Dardel, Y. Baer, Phys. Rev. Lett. **68**, 2656 (1992).
31. J.E. Han, M. Alouani, D.L. Cox, Phys. Rev. Lett. **78**, 939 (1997).
32. L. Duò *et al.*, Zeit. Phys. B **103**, 63 (1997).
33. C. Laubschat *et al.*, Phys. Rev. Lett. **65**, 1639 (1990).
34. L. Duò *et al.*, Phys. Rev. B **53**, 7030 (1996).
35. A fit to the Ce 3d Spectrum with  $|\varepsilon_f| = 2$  eV is also presented in: A. Kotani, T. Jo, J.C. Parlebas, Adv. Phys. **37**, 37 (1988).